

# Turbulent convection with time-dependent forcing

**J.J. Niemela, K.R. Sreenivasan**

The Abdus Salam ICTP, Strada Costiera 11, 34014 Trieste, Italy

E-mail: niemela@ictp.it

**Abstract.** A new technique is used to explore the structure of turbulent convecting flows. A sinusoidal temperature perturbation is superimposed on the bottom plate of a cylindrical convection cell filled with cryogenic helium gas and its decay is measured at the cell mid-height. The measurements allow the first dynamic estimate of the core part of the flow which conducts fluid effectively without any thermal resistance. The estimate is quantitatively consistent with recent numerical simulations.

## 1. Introduction

Thermal turbulence plays a major role in many large natural and engineering systems, from energy transport in stars to circulating currents in earth's atmosphere, oceans, mantle and core. A beginning point for its study is to reduce the problem to one that retains the essential physics, the so-called Rayleigh-Bénard convection (RBC). In RBC, a layer of fluid is contained between two horizontal and (typically) rigid plates (a heated bottom plate and a cooled top one). Sidewalls are usually ignored in analytical treatment, but cannot be similarly discarded in experiments.

In phenomenological models of turbulent convection, the fluid layer is divided into a boundary region and the bulk [1, 2] (though Ref. [3] introduced a third layer to account for what has often been regarded as the anomalous scaling of the heat transport). Here, we experimentally assess the structure of the flow by sinusoidally modulating the heating of the lower boundary about a mean value and observing the decay of the thermal wave at the mid-height of the cell. This modulation itself relies on the vanishing thermal impedance of the copper plates at low temperatures.

We can form a dimensionless measure of the vertical temperature difference resulting from applying heat to the bottom surface of a fluid layer as the Rayleigh number  $Ra \equiv \alpha \Delta T g H^3 / \nu \kappa$ , where  $\alpha$  is the isobaric thermal expansion coefficient of the fluid,  $\Delta T$  the temperature difference between the bottom and top plates separated by the vertical distance  $H$ , and  $g$  the acceleration due to gravity;  $\nu$  and  $\kappa$  are, respectively, the kinematic viscosity and thermal diffusivity of the fluid ( $\kappa \equiv k / \rho C_P$ , where  $k$  is the thermal conductivity,  $\rho$  is the density and  $C_P$  is the isobaric specific heat of the fluid). The ratio of the total heat flux to the pure conduction value (corresponding to the same realized temperature difference) is the Nusselt number,  $Nu$ , which is a power-law like function primarily of the Rayleigh number. The dynamical characteristics of the flow originate from plumes and thermals — blobs of fluid rising or falling from respectively unsteady diffusion region close to the heated or cooled surfaces. These elementary features of thermal turbulence self-organize to form a long-time coherent large-scale mean wind circulating along the periphery of the convection cell [4, 5, 6].

A fundamental notion of turbulent convection as  $Ra$  tends to infinity is that the temperature gradient vanishes in the bulk due to strong and rapid mixing, resulting in an effective thermal short-circuit between the two boundary regions, recently called the “superconducting” core [7]. The present measurements, already described in [7], were designed to shed light on this feature of turbulent convection. At moderately low  $Ra$ , we demonstrate the absence of the turbulent core, as expected, whereas for very high  $Ra$ , the existence of the core region can indeed be deduced and its spatial extent quantitatively measured. The results agree very well with profiles of the root-mean-square (rms) of the vertical temperature recently computed by Amati *et al.* [8]. The intervening fluid layer is substantially larger than the traditional thermal boundary layer associated with diffusive heat transport.

## 2. The experiment and the basic methodology

The apparatus is the same as that described earlier [10, 11, 9]. Briefly, it consists of a cylinder of 50 cm diameter with stainless steel sidewalls, 0.267 cm thick, containing helium gas near 5K, and surrounded by several radiation shields within a common vacuum space. The height could be adjusted to give different aspect ratios,  $\Gamma$ , defined as the ratio of the diameter to the height. The 3.8 cm thick top and bottom plates were fabricated from annealed OFHC copper, with thermal conductivity of the order of  $1 \text{ kW m}^{-1}\text{K}^{-1}$  at the measurement temperature.

The top plate of the cell was operated at a regulated constant temperature maintained by means of a resistance bridge and servo. The bottom plate was subject to a time-varying heat flux about a non-zero mean, such that its temperature is  $T_B(t) = \langle T_B \rangle + T_{B0} \cos(\omega t)$ , with the modulation frequency  $\omega = 2\pi f_M$ , where  $f_M$  has units of Hz and  $\langle \dots \rangle$  refers to averaging over integral periods of the modulation. We can define a dimensionless amplitude as  $\Delta_M = (T_{B0})_{rms} / \langle \Delta T \rangle$  where  $(T_{B0})_{rms}$  is the rms value of the measured amplitude of the temperature modulation at the bottom plate. In response to the modulation, a thermal wave propagates into the fluid at the forcing frequency  $\omega$  and is damped out exponentially with the rms value at a position  $z$  from the bottom wall given by

$$T_M^{CALC}(z, f_M) = (T_{B0})_{rms} \exp(-z/\delta_S), \quad (1)$$

where  $\delta_S$  is the so-called Stokes layer thickness, or the penetration depth, given by

$$\delta_S = \sqrt{\frac{\kappa^{eff}}{\pi f_M}}. \quad (2)$$

Here,  $\kappa^{eff}$  is an effective thermal diffusivity characteristic of the turbulent fluid. By the definition of the Nusselt number as the ratio of the effective thermal conductivity to its molecular value, it follows that

$$\kappa^{eff} = Nu(Ra) \cdot \kappa. \quad (3)$$

From the measured temperature amplitude of the thermal wave at the cell mid-height,  $T_M^{MEAS}(H/2, f_M)$ , and using (1)-(3), we can deduce the height of the layer  $\tilde{z}$  which all the attenuation occurs:

$$\tilde{z} = \ln\left(\frac{(T_{B0})_{rms}}{T_M^{MEAS}(H/2, f_M)}\right) \cdot \sqrt{\frac{Nu(Ra) \cdot \kappa}{\pi f_M}}. \quad (4)$$

At moderate  $Ra$  we should expect to get back  $\tilde{z} = H/2$  as we indeed do. It is more interesting, however, when the trivial answer is not produced, i.e., when  $\tilde{z} < H/2$ , signaling the formation of a core region in which the thermal wave essentially propagates without attenuation.

### 3. Results

Figure 1 shows temperature spectra obtained at the cell mid-height using a 250  $\mu\text{m}$  cubic germanium temperature sensor placed about 4 cm radially inboard from the sidewall. Temperature fluctuations were recorded at a rate 50 Hz using the off-balance signal from an audio frequency bridge circuit with lock-in detection. Here,  $\langle Ra \rangle = 3.4 \times 10^9$ ,  $f_M = 0.01$  Hz and  $\Delta_M = 0.05$ . The rms amplitude of the lower plate temperature modulation was  $(T_{B0})_{rms} = 0.00706$  K and the molecular thermal diffusivity of the fluid  $\kappa = 4.03 \times 10^{-2} \text{cm}^2/\text{s}$ . The rms amplitude of the thermal wave at the position of the sensor is  $7.5 \times 10^{-4}$  K, and we then obtain  $\kappa^{eff} = 3.893 \text{cm}^2\text{s}^{-1}$ . Taking its ratio to the molecular value  $4.034 \times 10^{-2} \text{cm}^2\text{s}^{-1}$ , and using Eqn. 3, gives  $Nu_\kappa = 96.5$ , which agrees quite well with the conventionally and simultaneously time-averaged measurement  $\langle Nu \rangle = 98.6$ , which itself is in excellent agreement with the steady heating result:  $Nu = 98.8$  demonstrating further that such modulation of the lower boundary temperature has negligible effect on the time-averaged heat transport.

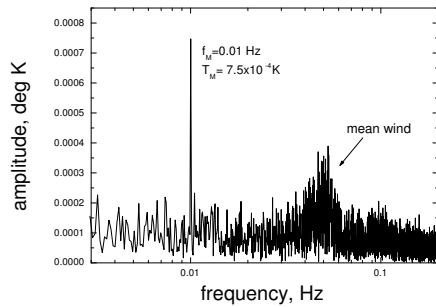


**Figure 1.** Amplitude spectra for  $\langle Ra \rangle = 3.4 \times 10^9$ ,  $f_M = 0.01$  Hz, and  $\Delta_M = 0.05$ . The position and amplitude of the spectral peak at  $f_P$  due to the mean wind remains essentially unchanged by the modulation.

The results of all experiments, conducted for for a wide variety of modulation frequencies and amplitudes and for both moderate and high  $Ra$ , as well as in an  $\Gamma = 4$  cell with  $H$  a factor 4 times smaller (with sensors near the sidewall and at the geometrical cell center) are shown in Table 1. We can easily summarize the situation at moderate  $Ra \sim 10^9$  by examining the column second from the right:  $\tilde{z}/H = 0.50 \pm 0.01$ , i.e., there is no evidence for a core.<sup>1</sup> Now let us consider the last two rows in Table 1 corresponding to high  $Ra \sim 10^{13}$ . In both cases the calculated wave amplitude is well below the noise floor, while the spectra give a measurable result over 2 orders of magnitude higher! Applying Eqn. 4, this demonstrates the formation of core region with negligible thermal resistance beginning at about 20% of the cell height.

**Table 1.** Parameters and measured values for modulation experiments (see text for details)

$\Gamma$	$Ra$	$f_M$ (Hz)	$(T_{B0})_{rms}$ (K)	$\kappa(\text{cm}^2/\text{s}^2)$	$\Delta_M$	$T_M^{meas}$ (K)	$T_M^{calc}$ (K)	$\tilde{z}/H$	pos.
4	$1.9 \times 10^9$	0.032	0.0229	$7.04 \times 10^{-3}$	0.15	$1.71 \times 10^{-3}$	$1.69 \times 10^{-3}$	0.50	side
4	$1.9 \times 10^9$	0.032	0.0229	$7.04 \times 10^{-3}$	0.15	$1.78 \times 10^{-3}$	$1.69 \times 10^{-3}$	0.49	center
1	$3.4 \times 10^9$	0.010	0.00706	0.04034	0.050	$7.5 \times 10^{-4}$	$7.7 \times 10^{-4}$	0.51	side
1	$3.5 \times 10^9$	0.0167	0.00676	0.04029	0.047	$4.1 \times 10^{-4}$	$3.9 \times 10^{-4}$	0.49	side
1	$3.5 \times 10^9$	0.07	0.00316	0.04032	0.022	— — —	$9.0 \times 10^{-6}$	— — —	side
1	$4.5 \times 10^{12}$	0.04	0.016	$7.93 \times 10^{-4}$	0.28	$1.5 \times 10^{-4}$	$7.8 \times 10^{-7}$	0.23	side
1	$1.0 \times 10^{13}$	0.025	0.009	$4.79 \times 10^{-4}$	0.22	$1.91 \times 10^{-4}$	$1.41 \times 10^{-6}$	0.22	side

<sup>1</sup> Note that the fifth and last entry at these  $Ra$  shows no measured amplitude as expected since the calculated value is below the noise threshold (see figure 1 for reference)!

Is this reasonable? Figure 2, taken from the simulation of Amati *et al.* [8], gives the answer. Plotted are the rms temperature profiles in turbulent convection.<sup>2</sup> The curves in Figure 2 correspond to  $Ra$  values that increase successively by an order of magnitude starting at  $Ra = 2 \times 10^9$ . We have marked by a horizontal arrow  $\tilde{z}/H$  corresponding to  $Ra = 1.9 \times 10^9$  terminating on the curve corresponding to  $Ra = 2 \times 10^9$ ; another horizontal arrow marks  $\tilde{z}/H$  for  $Ra = 10^{13}$  on the curve corresponding to the similar value  $Ra = 2 \times 10^{13}$ . It is clear by inspection of the rms profiles that there is no turbulent core region for  $Ra = 2 \times 10^9$ , consistent with our result of  $\tilde{z}/H = 0.5$ . The profile corresponding to  $Ra = 2 \times 10^{13}$ , on the other hand, shows an obvious core region starting at about 20% of the cell height, in very good agreement with our estimation.

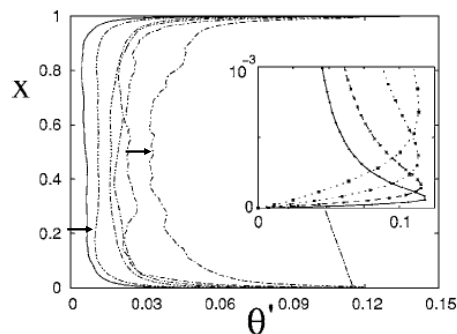


**Figure 2.** Profiles of the rms temperature from Amati *et al.* [8]. The curves from left to right vary by a factor of ten from  $2 \times 10^{14}$  to  $2 \times 10^9$ . The arrows indicate the estimate of  $\tilde{z}/H$  (ordinate “X”), which, for high  $Ra$ , coincide with the vanishing of the gradient in the profile.

#### 4. Summary

We have shown for a variety of modulation parameters in two cells of different aspect ratios, at both the sidewall and the cell center, that the measured damping of the oscillatory heating applied to the lower boundary can be used to quantify the extent of a “superconducting” core region in turbulent convection. The observations are in good quantitative agreement with the rms temperature profiles recently obtained by Amati *et al.* by numerically solving Boussinesq equations. This is the first time that a dynamic measurement has been used to explore the highly conducting core in turbulent convection at very high  $Ra$ .

##### 4.1. Acknowledgments

We thank Elettra Synchrotron Laboratory, Trieste, for providing laboratory space and support for these experiments.

- [1] L.N. Howard, *Proc. Nat. Acad. Sci.* **78**, 1981-1985 (1981).
- [2] W.V.R. Malkus, *Proc. R. Soc. Lond. A* **225**, 196 (1954).
- [3] B. Castaing, G. Gunaratne, F. Heslot, L. Kadanoff, A. Libchaber, A. S. Thomae, X.-Z. Wu, S. Zaleski, G. Zanetti, *J. Fluid Mech.* **204**, 1 (1989).
- [4] J.J. Niemela, L. Skrbek, K.R. Sreenivasan, R.J. Donnelly, *J. Fluid Mech.* **449**, 169-178 (2001).
- [5] X.-L. Qiu, P. Tong, *Phys. Rev. E* **64**, article no. 036304 (2001).
- [6] K.R. Sreenivasan, A. Bershadskii, J.J. Niemela, *Phys. Rev. E* **65**, paper no. 056306 (2002).
- [7] J.J. Niemela, and K.R. Sreenivasan, *Phys. Rev. Lett.* **100** 184502 (2008).
- [8] G. Amati, K. Koal, F. Massaioli, K.R. Sreenivasan, R. Verzicco, R. *Phys. Fluids* **17**, 121701 (2005).
- [9] J.J. Niemela, K.R. Sreenivasan, *J. Fluid Mech.* **557**, 411-422 (2006).
- [10] J.J. Niemela, L. Skrbek, K.R. Sreenivasan, R.J. Donnelly, *Nature* **404**, 837-840 (2000).
- [11] J.J. Niemela, K.R. Sreenivasan, *J. Fluid Mech.* **481**, 355-384 (2003).
- [12] M. S. Emran and J. Schumacher 2008 (Preprint); R. Verzicco, personal communication.

<sup>2</sup> While these simulations used  $\Gamma = 1/2$  to achieve the necessary high  $Ra$ , other simulations using the same code reveal no significant differences in the profiles between  $\Gamma = 1/2$  and  $\Gamma = 1$  for overlapping  $Ra$  and indeed, there is no reason to suspect that significant differences will arise at higher  $Ra$  [12].